Depth Profiling With Confocal Raman Microscopy, Part I

Raman microscopy is one of the techniques of choice for investigating heterogeneous systems on the micrometer scale. Part I of this two-part article series reviews the issues that must be considered to interpret confocal Raman data correctly.

Neil Everall

Raman spectroscopy is useful for studying the chemical structure of systems ranging from simple chemicals and plastics to biological structures. It is equally informative on physical properties such as crystal form, crystal size, molecular orientation, interactions and dynamics, and stress. For this reason, Raman microscopy is one of the techniques of choice for investigating heterogeneous systems on the micrometer scale. The Raman microscope focuses a laser beam down to a small volume (on the order of 1 μm^3 in air) and is operated readily in a confocal mode by placing an aperture at a back focal plane of the microscope (1). The aperture improves the lateral and axial spatial resolution of the microscope, allowing nondestructive depth profiling by acquiring spectra as the laser focus is moved incrementally deeper into a transparent sample (2). This approach often is termed "optical sectioning," as opposed to mechanically cutting a cross-section (microtomy) and scanning the laser beam laterally across the section. Because optical sectioning avoids the need for any sample preparation, numerous authors have applied it to the study of layered or graded systems and of phenomena at buried interfaces (2–10). Its noninvasive character makes it attractive particularly for the study of biological tissues (3, 10).

Confocal Raman microscopy can be applied in two ways. The first involves plotting the intensity of a component-specific band as a function of the distance from the sample surface. This reveals compositional or structural gradients as a depth profile. The second approach is to attempt to acquire a pure spectrum of a buried structure for identification purposes. Both of these applications require knowledge of the exact size and position of the microscope focal volume as it moves deeper into the sample, and this requires a detailed analysis that has been, until recently, largely ignored in the literature.

The purpose of this two-part article series is to review the issues that must be considered to interpret confocal Raman data correctly, and to present recent work demonstrating the extent to which depth resolution is degraded when focusing deep within a sample. The surface specificity of the technique also is discussed with particular regard to some unusual intensity variations that occur when focusing near a sample surface.

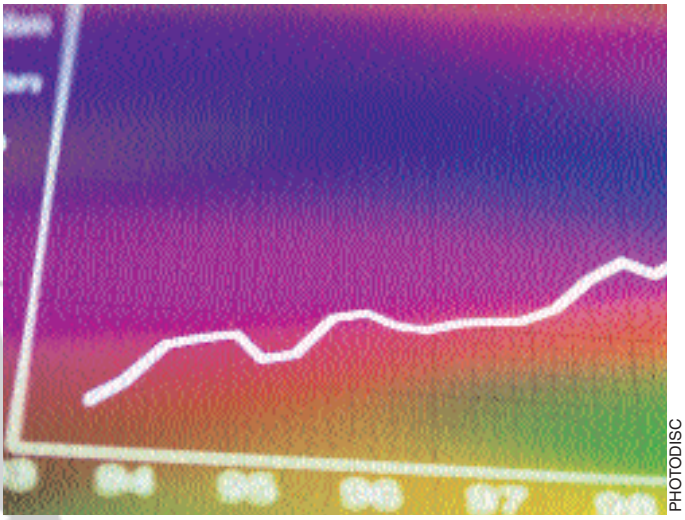

PHOTODISC

Metallurgical Objectives and Refraction

Almost every basic text or research publication that discusses the principles of confocal Raman microscopy includes a diagram similar to Figure 1 to indicate how a confocal aperture improves depth resolution. The depth resolution primarily depends upon two factors — the volume of the laser focus (Figure 1a) and how Raman photons generated within this volume are relayed back into the spectrometer via the confocal aperture (Figure 1b). The laser focus appears at point C in Figure 1a. In nontransparent media, scattering makes the focus more diffuse, spreading from A to B and degrading the depth resolution. Placing an aperture at a back focal plane of the system should improve the depth resolution by only transmitting those rays that originate near point C.

According to Juang et al. (11), the limiting resolution DR is given by equation 1, where n is the refractive index of the immersion medium, λ is the laser wavelength, and NA is the numerical aperture of the focusing lens.

$$DR = \frac{2.2n\lambda}{\pi(NA)^2} \qquad [1]$$

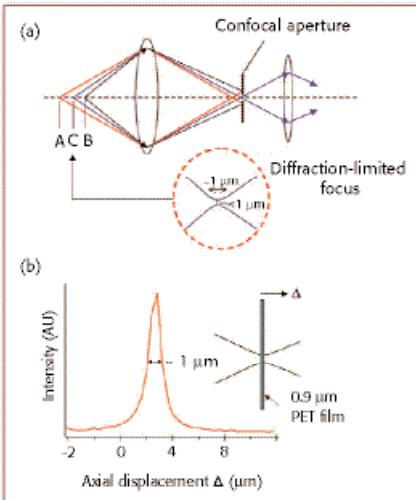

Figure 1. (a) Schematic showing operation of a confocal aperture, blocking radiation from points A and B and allowing light from point C to pass to the spectrometer, thereby improving axial resolution. (b) Simplified test of axial resolution, translating a thin-film PET sample through the laser focus.

Equation 1, taken literally, implies that the depth resolution improves monotonically as NA increases. For example, with a 514.5-nm laser and an objective with NA = 0.95, the expected depth resolution is 0.6 µm (12). Tabaksblat et al. (4) made calculations and practical determinations of the depth resolution as a function of the numerical aperture of the objective, the microscope magnification, and the size of the pinhole, and concluded that a resolution of ~2 µm was obtained with a 100X objective and a 100-µm pinhole. On the basis of this kind of analysis one would expect that confocal Raman microscopy can be used to obtain depth profiles with an axial resolution determined only by the objective numerical aperture, the magnification, and the pinhole size, irrespective of how deeply one focuses below the sample surface. Unfortunately, the simple tests that usually are applied to test the depth resolution reinforce this incorrect assumption and give misleading results. These tests involve measuring the intensity of Raman scatter of either a very thin or opaque sample as it is translated through the laser focus along the beam propagation axis (usually the surface normal). Throughout this paper we define the sample displacement along this axis by the symbol Δ, which we term the axial displacement. In practical terms it corresponds to the displacement of the microscope stage, in micrometers, relative to the position where the laser is focused on the sample top surface. If Δ = 0, the laser beam is focused on the air–sample interface, and positive values of Δ imply sample movement opposite to the beam propagation direction (that is, moving the laser focus into the sample). Figure 1b shows the response as a 0.9-µm thick film of PET (polyethyleneterephthalate) was translated through the focus of a 633-nm laser beam focused by a 0.9-NA, 100X metallurgical objective. The full width at half maximum (fwhm) of the profile was 1.1 µm, implying excellent depth resolution for this instrumental configuration. For a very thin or opaque sam-

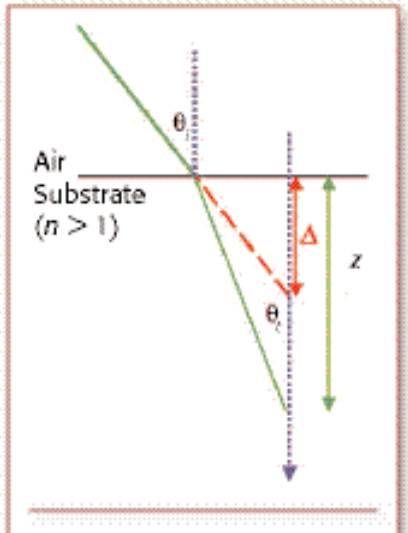

Figure 2. Schematic showing the shift in laser focus due to refraction, which can be quantified using Snell's Law.

ple, this essentially maps out the axial intensity profile in air (not as it appears deep within a transparent sample).

Unfortunately, the configurations shown in Figure 1 are not representative of confocal Raman microscopy as it is normally practiced — that is, with a metallurgical objective focused into a thick (>1 μm) sample immersed in air. Metallurgical objectives are designed to focus on the surface of opaque samples, but when focusing beneath the surface of a sample with n >1, the light rays are refracted and the laser intensity distribution becomes shifted and distorted. Figure 2 illustrates the problem. Any ray that passes into a sample immersed in air will suffer refraction through an angle determined by Snell's Law: $\sin \theta_i / \sin \theta_t = n$, where θ_i and θ_t are the angles of incidence and transmission with respect to the surface normal. In the absence of refraction the ray would come to a focus at a distance Δ below the sample/air interface, but when n >1, the focal point lies deeper, at z. The ratio of refracted and nonrefracted focal depths is given by $z/\Delta = \tan \theta_i / \tan \theta_t$, which tends to n as θ_i tends to zero. Therefore, z/Δ has a minimum value of n, and increases as θ_i becomes larger. To correctly interpret confocal Raman depth profiles one obviously must take this spread in focal positions into account.

Several issues must be considered to interpret confocal Raman data correctly.

The first step in analyzing the importance of this effect is to calculate the focal depth as a function of the radial coordinate of each ray leaving the objective (see Figure 3). Neglecting diffraction, this has a simple analytical solution (13) (see equation 2).

Here r_k is the radius of origin of the k^{th} ray, NA is the numerical aperture of the objective ($n \sin \theta_i$), r_{max} is the maximum radius accessible to a ray, the fractional radius $m = r_k / r_{max}$, and Δ is defined above.

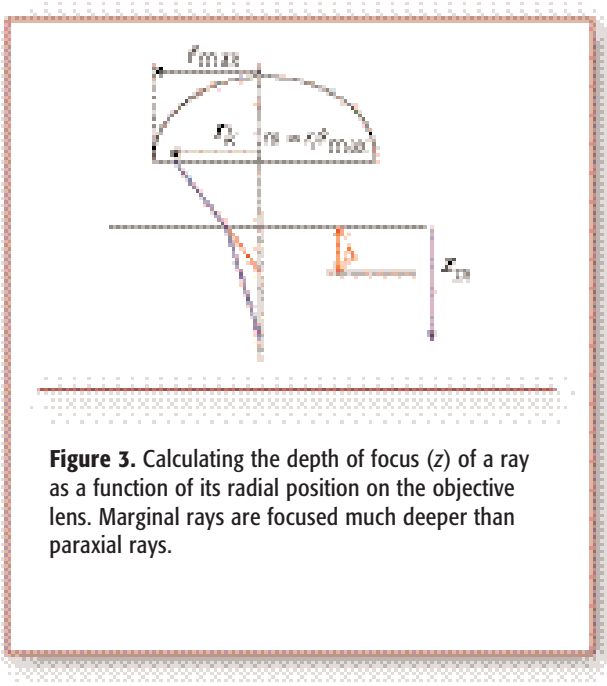

Figure 3. Calculating the depth of focus (z) of a ray as a function of its radial position on the objective lens. Marginal rays are focused much deeper than paraxial rays.

Equation 2 gives the true point of focus z_m for a ray originating at m. It is obvious that rays that originate at different radii on the objective are focused to a different depth, (spherical aberration). In the paraxial limit ($m \rightarrow 0$), then $z_0/\Delta = n$, in agreement with the discussion of Figure 2 above. To summarize, the ratio of the refracted and non-refracted focal depths (z_m/Δ) increases with both m and NA, so one expects the spherical aberration

$$z_m = \Delta\left[\frac{r_k^2 \mathrm{NA}^2 (n^2-1)}{r_{max}^2 (1-\mathrm{NA}^2)} + n^2\right]^{1/2} = \Delta\left[m^2 \cdot \frac{\mathrm{NA}^2 (n^2-1)}{(1-\mathrm{NA}^2)} + n^2\right]^{1/2} \quad [2]$$

$$\mathrm{DR} = z_{m=1} - z_{m=0} = \Delta\left[\left[\frac{\mathrm{NA}^2 (n^2-1)}{(1-\mathrm{NA}^2)} + n^2\right]^{1/2} - n\right] \quad [3]$$

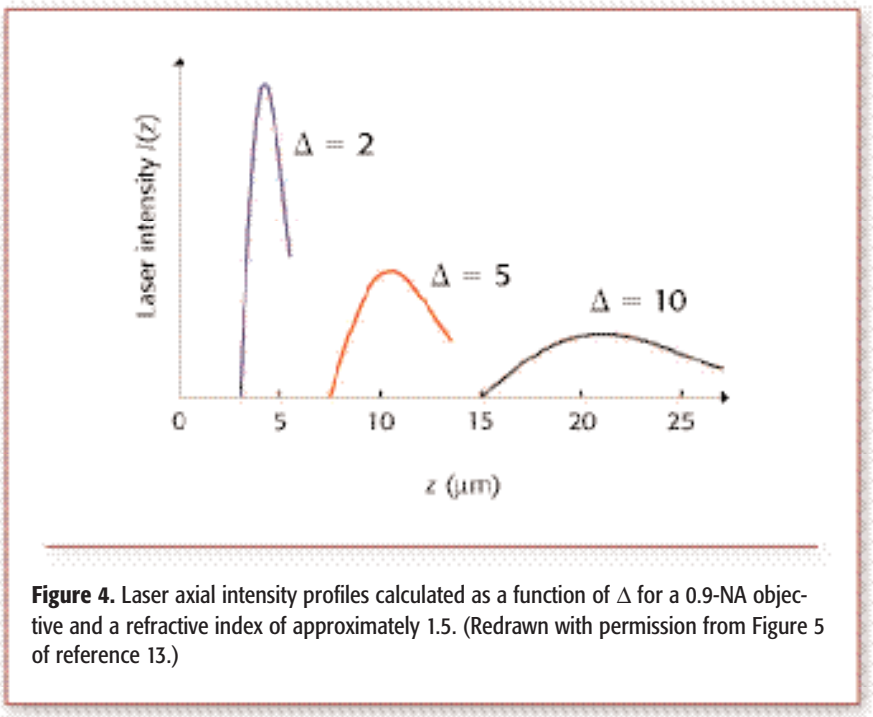

Figure 4. Laser axial intensity profiles calculated as a function of Δ for a 0.9-NA objective and a refractive index of approximately 1.5. (Redrawn with permission from Figure 5 of reference 13.)

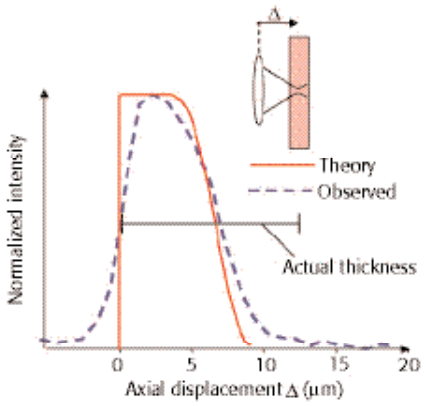

Figure 5. Measured and calculated intensity response for a 12-μm thick PET film as a function of axial displacement Δ. Note the apparent compression of the depth scale compared to the true thickness. (Redrawn with permission from Figure 3 of reference 14.)

to be worsened at large NA values.

Defining the depth resolution (DR) as the difference between the maximum and minimum depths of focus, DR = $z_{m=1} - z_{m=0}$ (see equation 3).

Equation 3 implies that the depth resolution should degrade linearly as we focus deeper below the surface (Δ). It also implies that increasing the numerical aperture yields a worse depth resolution (DR tending to infinity as NA approaches 1). This runs counter to the effect of diffraction (equation 1), and if the NA is reduced too much then broadening due to diffraction will dominate.

In brief, the important consequences of equations 2 and 3 are that we always are focused deeper than the microscope scale would indicate, and the axial laser focus broadens upon moving deeper into the sample. Assuming a Gaussian laser intensity profile across the microscope objective we can use equation 2 to map the radial intensity distribution across the lens into the axial intensity distribution ($I(z)$), as a function of Δ (13). Figure 4 shows the broadening of $I(z)$ with increasing Δ. When focusing to a nominal depth Δ = 10 μm with a 0.9-NA objective, one actually illuminates between 15 and 27 μm below the sample surface. This means that great care must be exercised when interpreting confocal Raman intensity profiles. The consequences of neglecting these effects have been discussed in detail elsewhere (13, 14).

Figure 5 illustrates the practical consequences using the simplest possible system, a single layer of a uniform polymer film. The raw intensity profile incorrectly indicates that the film thickness is ~6 μm, rather than the correct value of 12 μm. This is in quite

good agreement with the calculated response curve. Calculated intensity profiles generally have been shown to be in good agreement with the observed data for a number of coated films and laminates (13, 14), indicating that this very simple model provides a reasonable predictive tool for computing the expected profile. This foreshortening of the raw depth profile has been confirmed subsequently by a number of workers using similar experiments; only a few examples are quoted here for reference purposes (8, 15–17). In summary, refraction results in the depth of buried structures being underestimated grossly in a raw intensity depth profile (typically by a factor of 2 with a 0.9-NA objective, the exact factor can be calculated as a function of NA [13]).

BECAUSE A SIMPLE SCALING FACTOR CANNOT ALWAYS BE APPLIED TO CALCULATE THE TRUE THICKNESS OF A SAMPLE'S BURIED LAYERS, PROPER MODELING OF THE CONFOCAL PROFILE IS RECOMMENDED.

Calculating the thickness of deeply buried layers is not trivial because we cannot always apply a simple scaling factor to calculate the true thickness. In earlier papers it was stated that with a high NA objective, both the observed position and the thickness of buried layers are underestimated badly, each by a factor of ~2 (13,14). In fact, as will be discussed in Part II, this is not always correct; the observed thickness depends upon the thickness of the layer and its depth below the surface, and can appear to be too thick or too thin. In other words, the apparent depth resolution is a function of depth within the sample. Thus proper modeling of the confocal profile, rather than simple scale correction, is recommended.

References

1. P. Dhamelincourt, "Raman Microscopy," *Handbook of Vibrational Spectroscopy,* vol. 2, J.M. Chalmers and P. R. Griffiths, Eds. (John Wiley & Sons, Chichester, 2002), pp. 1149–1428.
2. P.M. Fredericks, "Depth Profiling by Microspectroscopy," *Handbook of Vibrational Spectroscopy*, vol. 2, J.M. Chalmers and P. R. Griffiths, Eds. (John Wiley & Sons, Chichester, 2002), pp. 1493–1507.
3. C. Xiao, C.R. Flach, C. Marcott, and R. Mendelsohn, *Appl. Spectrosc.* **58**, 382 (2004).
4. R. Tabaksblat, R.J. Meier, and B.J. Kip, *Appl. Spectrosc.* **46**, 60 (1992).
5. S. Hajatdoost and J. Yarwood, *Appl. Spectrosc.* **50**, 558 (1996).
6. C. Sammon, S. Hajatdoost, P. Eaton, C. Mura, and J. Yarwood, *Macromol. Symp*. **141**, 247 (1999).
7. K.P.J. Williams, G.D. Pitt, D.N. Batchelder, and B.J. Kip, *Appl. Spectrosc.* **48**, 232 (1994).
8. H. Reinecke, S.J. Spells, J. Sacristan, J. Yarwood, and C. Mijangos, *Appl. Spectrosc.* **55**, 1660 (2001).
9. N. Everall, K. Davis, H. Owen, M.J. Pelletier, and J. Slater, *Appl. Spectrosc.* **50**, 388 (1997).
10. P.J. Caspers, G.W. Lucassen, and G.J. Puppels, *Biophys. J.* **85**, 572 (2003).
11. C.B. Juang, L. Finzi, and C.J. Bustamante, *Rev. Sci. Instrum*. **59**, 2399 (1988).
12. J. Barbillat, P. Dhamelincourt, M. Delhaye, and E. da Silva, *J. Raman Spectrosc*. **25**, 3 (1994).
13. N.J. Everall, *Appl. Spectrosc.* **54**, 773 (2000).
14. N.J. Everall, *Appl. Spectrosc.* **54**, 1515 (2000).
15. J. Vyorykka, M. Halttunen, H. Iitti, J. Tenhunen, T. Vuorinen, and P. Stenius, *Appl. Spectrosc.* **56**, 776 (2002).
16. L. Baia, K. Gigant, U. Posset, G. Schottner, W. Kiefer, and J. Popp, *Appl. Spectrosc.* **56**, 536 (2002).
17. O.S. Fleming, K.L.A. Chan, and S.G. Kazarian, *Vib. Spectrosc.* **35**, 3 (2004). ■

Neil Everall is a research associate with the Measurement Science Group at ICI plc (U.K.). E-mail the author at: neil_everall@ici.com.